



Research Article

Comparative evaluation of experimental ejector refrigeration system for different operating configurations

Batuhan ÜGÜDÜR¹, Mehmet DİREK^{2,*}

¹Department of Energy Systems Engineering, Institute of Graduate Studies, Yalova University, Yalova, 77200, Türkiye

²Department of Energy Systems Engineering, Faculty of Engineering, Yalova University, Yalova, 77200, Türkiye

ARTICLE INFO

Article history

Received: 12 December 2022

Revised: 12 March 2023

Accepted: 15 April 2023

Keywords:

Cooling Capacity; COP; Dual Evaporator; Ejector

ABSTRACT

In this study, a comparative performance evaluation of an experimental ejector refrigeration system was conducted for various operating modes. The experimental setup was operated in different modes: conventional vapour compression refrigeration (CVCR), conventional dual-evaporator system (CDES), and dual-evaporator ejector system (DEES). The system was tested under different operating conditions, including varying condenser temperatures and mass flow rates. The results of the evaluation showed that the highest total cooling capacity and coefficient of performance (COP) were achieved in the DEES mode, while the lowest total cooling capacity was observed in the CDES mode. The lowest compressor power was calculated when the system was operated in DEES mode. When the condenser temperature was 33°C, the compressor power obtained in the DEES mode was 22.7%, 5.4%, and 17.7% lower than that of the CVCR_A, CVCR_B, and CDES modes, respectively. In conclusion, the performance of the ejector-operated system was found to be superior to the other configurations, and the ejector contributed positively to the system performance.

Cite this article as: Ügüdür B, Direk M. Comparative evaluation of experimental ejector refrigeration system for different operating configurations. J Ther Eng 2024;10(2):321–329.

INTRODUCTION

Vapour compression refrigeration (VCR) cycles are commonly used for cooling, heating, ventilation, and other air conditioning applications in buildings. The energy consumption required to run these systems accounts for approximately 20% of all energy consumption [1]. Energy prices have significantly increased due to high natural gas and fuel prices, as well as environmental concerns. Therefore, it is crucial to utilize refrigeration systems with lower energy consumption

values while maintaining their performance. The throttling process in conventional VCR (CVCR) and heat pump (HP) systems results in irreversibilities and energy losses. These losses can be recovered by using an ejector [2,3]. The addition of an ejector and a liquid-vapour separator to the CVCR allows the system to operate using an ejector and enhance the efficiency of the CVCR or HP system [4,5]. In the literature, studies have been carried out on the use of ejectors in refrigeration systems [6,7]. Due to inefficiencies in operating the liquid-vapour separator, an alternative approach is to

*Corresponding author.

*E-mail address: mehmet.direk@yalova.edu.tr

This paper was recommended for publication in revised form in Editor-in-Chief Ahmet Selim Dalkılıç



use dual evaporators in an ejector refrigeration system [8]. In addition, different system configurations can be created for two-evaporator systems using ejectors [9]. According to a study by Geng et al. [10], the COP obtained from DEES was reported to be 16% to 30% higher than that of the conventional system. Another study by Kim et al. [11] tested an experimental bi-evaporator refrigeration system that used an ejector with different geometries. The COP of the DEES was found to diminish as the entrainment ratio (ER) increased, owing to the decrease in pressure lifting ratio. In a theoretical study, Gao et al. [12] compared the performance of ejector refrigeration systems and found that the COP increased by 36% when an ejector was used. Liu et al. [13] tested a dual ejector refrigeration cycle using CO₂ and found that the COP value was 15% to 27% higher than that obtained from a conventional system. Wang et al. [14] suggested using an ejector in a HP system and found that when R22, R290, and R32 were used in the system, there was an increase of 2.6% to 3.1%, 3.2% to 3.7%, and 2.9% to 3.1% in COP compared to a conventional HP. Wang et al. [15] conducted a study on the use of ejector in a HP system. The new system was compared to a conventional HP using R1234yf. The COP was found to be improved by 24.93% with the HP using an ejector compared to the VCR system. Chen et al. [16] investigated an ejector compression HP system designed for water heating. The proposed system resulted in 24.1% and 29% higher COP values for heating compared to HP with ejector and air source HP, respectively. Alkhulaifi et al. [17] investigated the DEES

and found that it provides an efficiency advantage compared to CVCR. Iskan and Direk [18] tested a DEES system using six different refrigerants with low Global Warming Potential (GWP) as an alternative to R134a. The study concluded that R516A is the most suitable refrigerant alternative to R134a.

In the literature, it is observed that there are not many experimental studies investigating ejector cooling systems operating different modes. Therefore, in this study, a refrigeration system was experimentally tested in various operating modes with and without an ejector. An experimental system equipped with dual evaporators and ejectors was created to test its performance under different configurations. The system was operated with various combinations, and the impact of the ejector on the system performance parameters (compressor power, cooling capacity of evaporator#1, total cooling capacity, and COP) was determined for different configurations under various condensing temperatures and mass flow rates.

EXPERIMENTAL SYSTEM

The experimental system is designed to operate in four different modes: CVCR_A, CVCR_B, CDES, and DEES. Control valves and by-pass lines are added to the system to enable operation in different modes. The test rig employs a semi-hermetic compressor (Danfoss brand, volume: 30.23 cm³ rev⁻¹). The positions of the equipment in the system are illustrated in Figure 1.

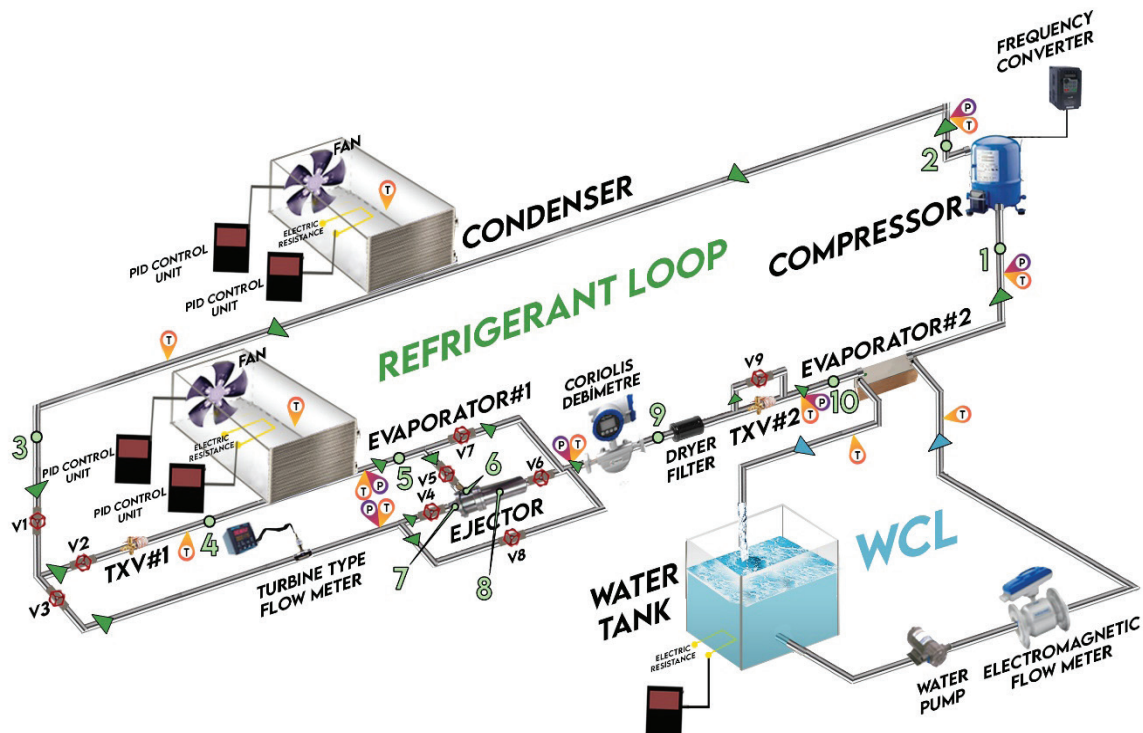


Figure 1. The schematic of the ejector refrigeration cycle [19].

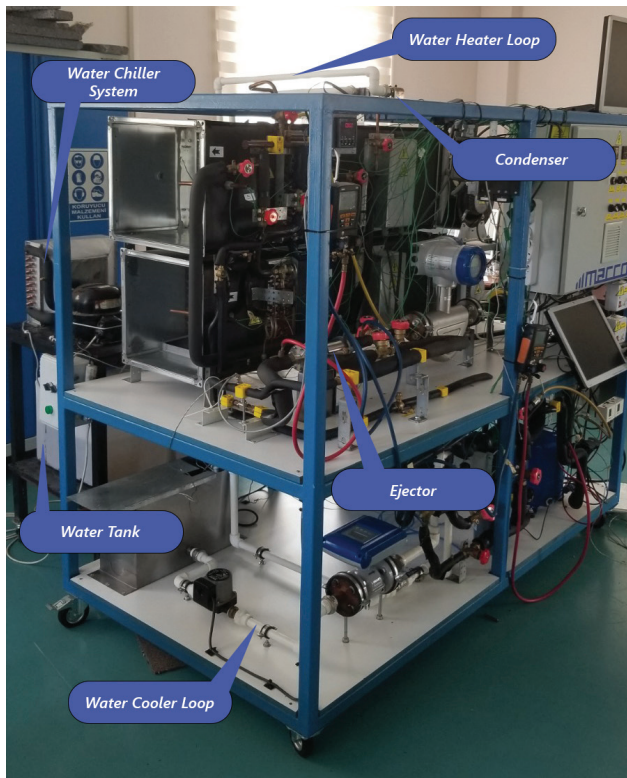


Figure 2. Experimental setup.

A 3D schematic diagram and a photo of the experimental setup are indicated in Figure 1 and Figure 2. Apparatus and measuring devices are mounted on an experimental-setup constructed using metal profiles for support and stability. The condenser (357mm x 330mm x 132mm) and evap#1 (300mm x 305mm x 110mm) are positioned in the upper part of the experimental-setup within the air channels. A plate type heat-exchanger, which was used as evap#2, was connected to a water cooling loop (WCL) and located in the lower part of the experimental rig. The WCL consists of a plate heat exchanger, a water tank, a pump, and an electromagnetic flow meter. All apparatus in the WCL was connected using plastic tubes. A Coriolis-flow-meter was used at the ejector outlet and a turbine-type-flow meter was placed at the second inlet of the ejector. The data

acquisition system was placed in the upper part of the test rig. Temperature measurements were taken at the inlet and outlet points of all equipment with K-type thermocouples. In order to measure the refrigerant pressures, digital manometers and pressure transmitters were used. Ranges and accuracies of the measurement devices are displayed in the Table 1.

The geometry and dimensions of the ejector used can be found in our previous work [20]. Once the refrigerant exits the compressor as high-pressure superheated vapour, it condenses in the condenser, and then splits into two streams at the exit of the condenser. The first stream enters the ejector through its primary inlet, where it accelerates as it passes through the nozzle section and experiences a pressure drop. In order for the system to operate effectively, the pressure at this point must be lower than the pressure of the refrigerant flow vaporizing in evap#1, which is achieved by the pressure difference created by the TXV. Consequently, the refrigerant flow in the form of superheated vapour at the exit of evap#1 (second stream) is drawn into the mixing chamber of the ejector. The two streams then mix in the chamber and expand and slow down while their pressure increases in the diffuser. At this point, the pressure should be higher than the pressure at the second inlet of the ejector and lower than the pressure at the first inlet. Finally, the refrigerant flow in the form of a liquid-vapour mixture exits the ejector and evaporates in evap#2 before returning to the compressor.

Thermodynamic Analysis

Equations were used to determine the performance parameters in different system configurations with and without ejector were given in Table 2. The ranges of uncertainties of the experimental parameters are presented in Table 3.

Experimental Procedure

In the experimental study, 1000 g of R134a was charged into the system. Desired air flow rates and temperatures were generated with the electric heaters and fans installed in the channels. After the experimental conditions were established, the experiments were initiated, and data from measurements were recorded on the computer once the system reached a steady state. Furthermore, the

Table 1. Parameters of the measurement devices [19].

Measurement	Device	Range	Accuracy
\dot{m}_r	Turbine-flow-meter	0.2 to 1.2 kg/s	± 0.1 %
V_{air}	Anemometer	0.4 - 20 m.s ⁻¹	± 2.0 %
\dot{m}_r	Coriolis-flow-meter	0 - 5 kg/s	± 0.05 %
Pressure	Electronic-manifold	-1 - 60 bar	± 0.5 %
Temperature	K-type Thermocouple	-100 -1370 °C	± 1.5 °C

Table 2. Thermodynamic and uncertainty equations [19].

	CVCRA	CVCRB	CDES	DEES
Evap#1 cooling capacity ($\dot{Q}_{evap\#1}$)	$= (h_{10} - h_1)\dot{m}_1$	-	$= (h_5 - h_4)\dot{m}_1$	$= (h_5 - h_4)\dot{m}_2$
Total cooling capacity ($\dot{Q}_{evap,total}$)	$= \dot{Q}_{evap\#1}$	$= \dot{Q}_{evap\#2}$	$= (\dot{Q}_{evap\#1} + \dot{Q}_{evap\#2})$	$= (\dot{Q}_{evap\#1} + \dot{Q}_{evap\#2})$
Compressor power (\dot{W}_{comp})	$= (h_2 - h_1)\dot{m}_1$	$= (h_2 - h_1)\dot{m}_1$	$= (h_2 - h_1)\dot{m}_1$	$= (h_2 - h_1)\dot{m}_1$
COP	$= \frac{\dot{Q}_{evap\#1}}{\dot{W}_{comp}}$	$= \frac{\dot{Q}_{evap\#2}}{\dot{W}_{comp}}$	$= \frac{\dot{Q}_{evap,total}}{\dot{W}_{comp}}$	$= \frac{\dot{Q}_{evap,total}}{\dot{W}_{comp}}$
Uncertainty (U_y)	$= \sqrt{\sum_{i=1}^n \left(\frac{\partial y}{\partial x_i} u_{x_i} \right)^2}$			

Table 3. Range of uncertainties of experimental parameters.

Experimental parameters	Range of uncertainties
$\dot{Q}_{evap\#1}$	% 0.71 – 0.85
\dot{W}_{comp}	% 0.25 – 0.27
$\dot{Q}_{evap,total}$	% 0.37 – 0.42
COP	% 3.75 – 4.50

Table 4. Experimental conditions.

T_{water} of evap#2 (°C)	25
V_{air} of evap#1 (m s ⁻¹)	1.2
$T_{ambient}$ (°C)	21
\dot{m}_{water} of evap#2 (kg s ⁻¹)	0.294
ER	0.5

Table 5. Active and passive apparatus in condenser temperature experiments.

	Cond#1	Cond#2	Evap#1	Evap#2	TXV#1	TXV#2	Ejector
CVCRA	+	-	+	-	+	-	-
CVCRB	+	-	-	+	-	+	-
CDES	+	-	+	+	+	-	-
DEES	+	-	+	+	+	-	+

parameters that were kept constant throughout the experiments are listed in Table 4. Active and passive equipment for using different configurations of the system in condenser temperature (ct) experiments were shown in Table 5. Active equipment is demonstrated as (+) and passive equipment as (-). As seen in Table 5, in CVCR_A evap#1 is active, whereas in CVCR_B, evap#2 is active.

RESULTS AND DISCUSSION

Effect of Condenser Temperatures on the Performance Parameters

The results obtained from the experiments performed in CVCR_A, CVCR_B, CDES and DEES modes are presented

comparatively in the following section. The variation of the mass flow rates (\dot{m}_r) with respect to ct is given in Figure 3a. It was determined that the \dot{m}_r increased for all modes with the increase of ct. The lowest \dot{m}_r was obtained when the system was operated as CDES. For example, when the ct is 36°C, the mass flow rate obtained from CDES was found to be 43.9%, 33% and 7.7% lower compared to the DEES, CVCR_A, and CVCR_B. When the system is operated in CDES mode, the evaporation temperatures in evap#1 and refrigerant vapour densities decreased. Therefore, when the system was operated as CDES, the lowest \dot{m}_r was measured. The velocity of the refrigerant entering the ejector's primary inlet increases when the ejector is activated, leading to an increase in the \dot{m}_r . Compressor inlet pressure increased in

all configurations with increasing ct (Figure 3b). The lowest compressor inlet pressure was obtained in the CDES mode since the ejector was by-passed and a throttling device was used. For example, when ct was 39°C , the $P_{\text{comp-inlet}}$ obtained from the CDES was lower than the other considered configurations. Since the refrigerant passing from the mixing chamber of the ejector to the diffuser passes through a larger cross-sectional area, its pressure increases. As a result, the highest compressor inlet pressure value was reached in the system using ejector (DEES). This shows that the contribution of the ejector is consistent with the literature [11].

The variation of the compressor power (\dot{W}_{comp}) obtained in four different modes depending on the ct is given in Figure 4a. \dot{W}_{comp} increased with raising ct . \dot{W}_{comp} increased as the ct increased due to the increase in the refrigerant flow rate. The lowest compressor power were obtained from the

CDES mode. The highest compressor power were measured in DEES mode. Due to the high flow rates, the highest compressor power resulted in DEES mode. As shown in Figure 4b, the $\dot{Q}_{\text{evap}\#1}$ increased with the increase of ct . As evaporator#1 is inactive in CVCR_B mode, its performance is not depicted in Figure 3b. At a ct of 39°C , the $\dot{Q}_{\text{evap}\#1}$ measured in the DEES mode was found to be 23.7% lower than that of the CDES mode and 53.5% lower than that of the CVCR_A mode.

As the ct increased, the total \dot{Q}_{evap} increased in all configurations. The lowest $\dot{Q}_{\text{evap},\text{total}}$ value was obtained when the system was operated in CDES mode (Figure 5a). For instance, when the ct was 36°C , the $\dot{Q}_{\text{evap},\text{total}}$ obtained from CDES was 45.6%, 32.4%, and 8.3% lower than the values obtained from DEES, CVCR_A , and CVCR_B modes, respectively. Due to the high mass flow rates, the highest total

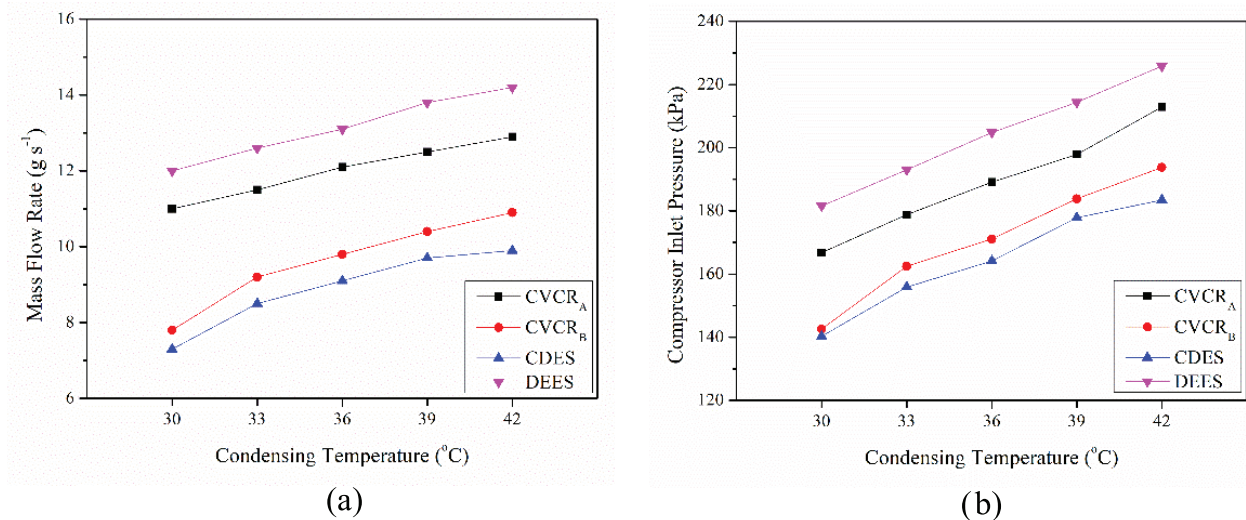


Figure 3. Changes in mass flow rates (a) and compressor inlet pressure (b) as a function of condensing temperature.

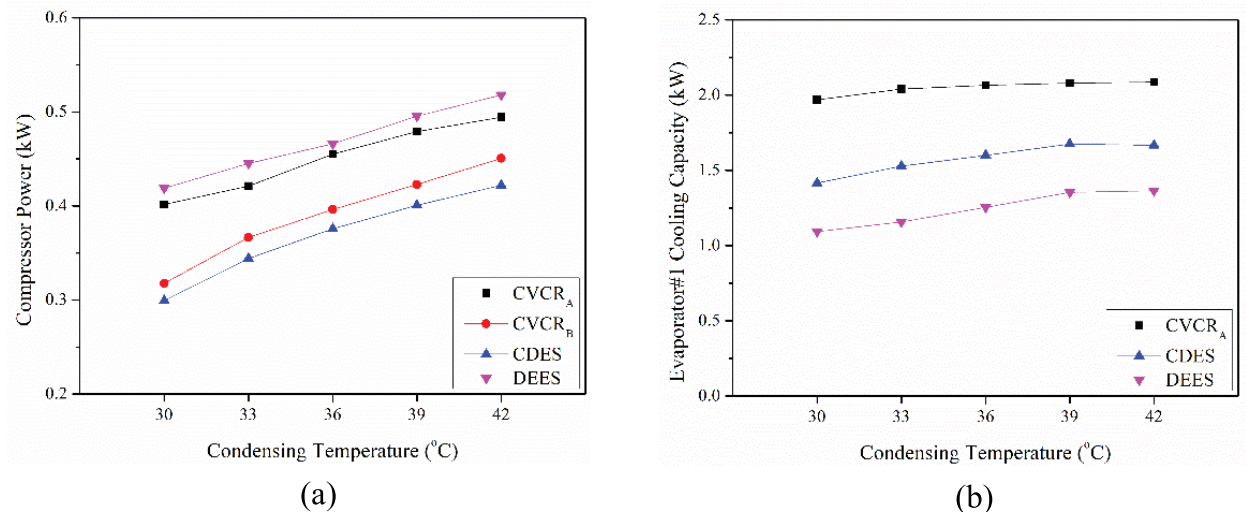


Figure 4. Changes in mass flow rates (a) and compressor inlet pressure (b) as a function of condensing temperature.

$\dot{Q}_{evap, total}$ was calculated in the DEES mode, while the lowest was obtained in the CDES mode. The COP values decreased in all configurations with increasing ct (Figure 5b), which is consistent with the findings reported by Geng et al. [10] and Gao et al. [12]. The COP value decreased due to the increase in compressor power being greater than the increase in the $\dot{Q}_{evap, total}$. The subcooling degrees dropped with increasing ct in all configurations (Figure 5c). The highest subcooling was obtained from the CDES mode. Since the condenser power per unit mass refrigerant is constant, a lower \dot{W}_{comp} input

results in a higher degree of subcooling. Therefore, the configuration with the lowest \dot{W}_{comp} (CDES) yielded the highest degree of sub-cooling.

Effect of Mass Flow Rates on the Performance Parameters

In this section, changes in experimental parameters due to changes in mass flow rates when the system is operated in different configurations are analysed comparatively. Active and passive devices are given in Table 6.

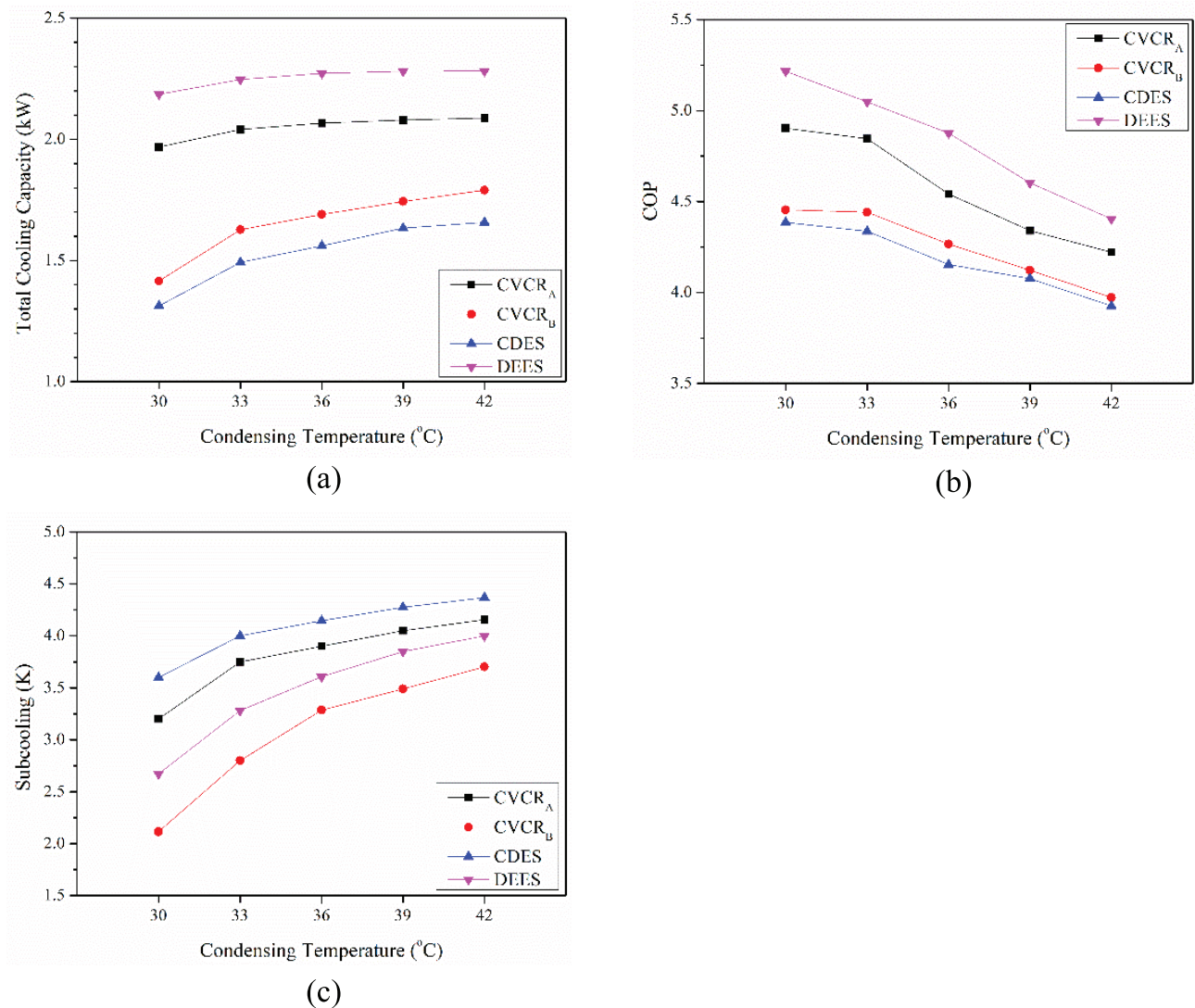


Figure 5. Changes in total cooling capacity (a) COP (b) and subcooling (c) as a function of condensing temperature.

Table 6. Active and passive apparatus in \dot{m}_r experiments.

	Cond#1	Cond#2	Evap#1	Evap#2	TXV#1	TXV#2	Ejector
CDES	+	-	+	+	+	-	-
DEES	+	-	+	+	+	-	+

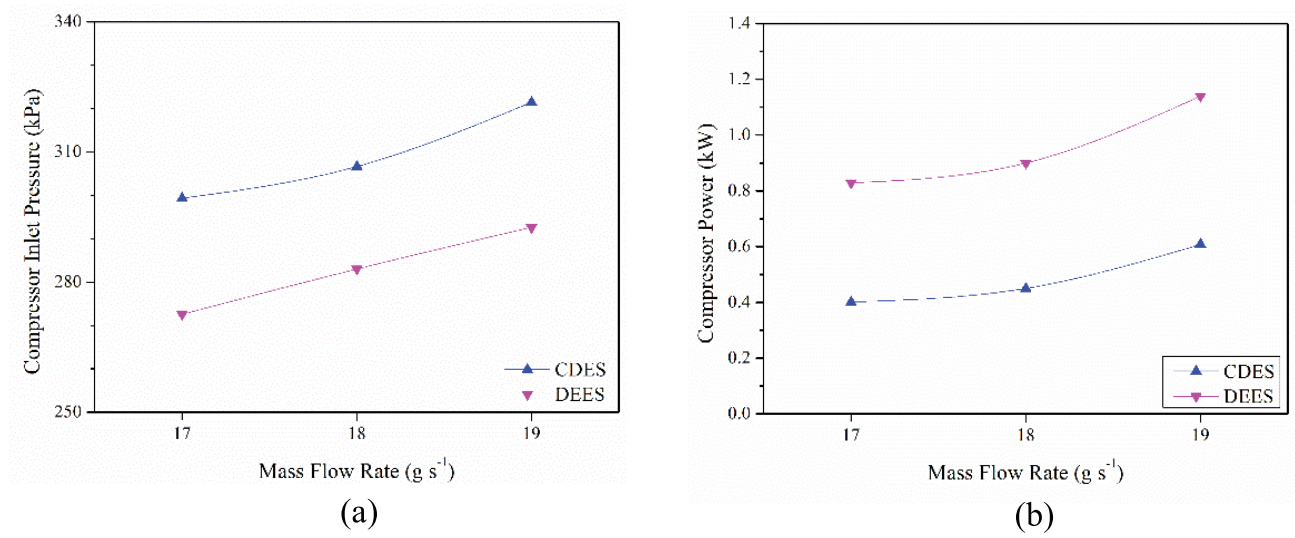


Figure 6. Changes in condenser inlet temperature (a) and compressor power (b) as a function of mass flow rates.

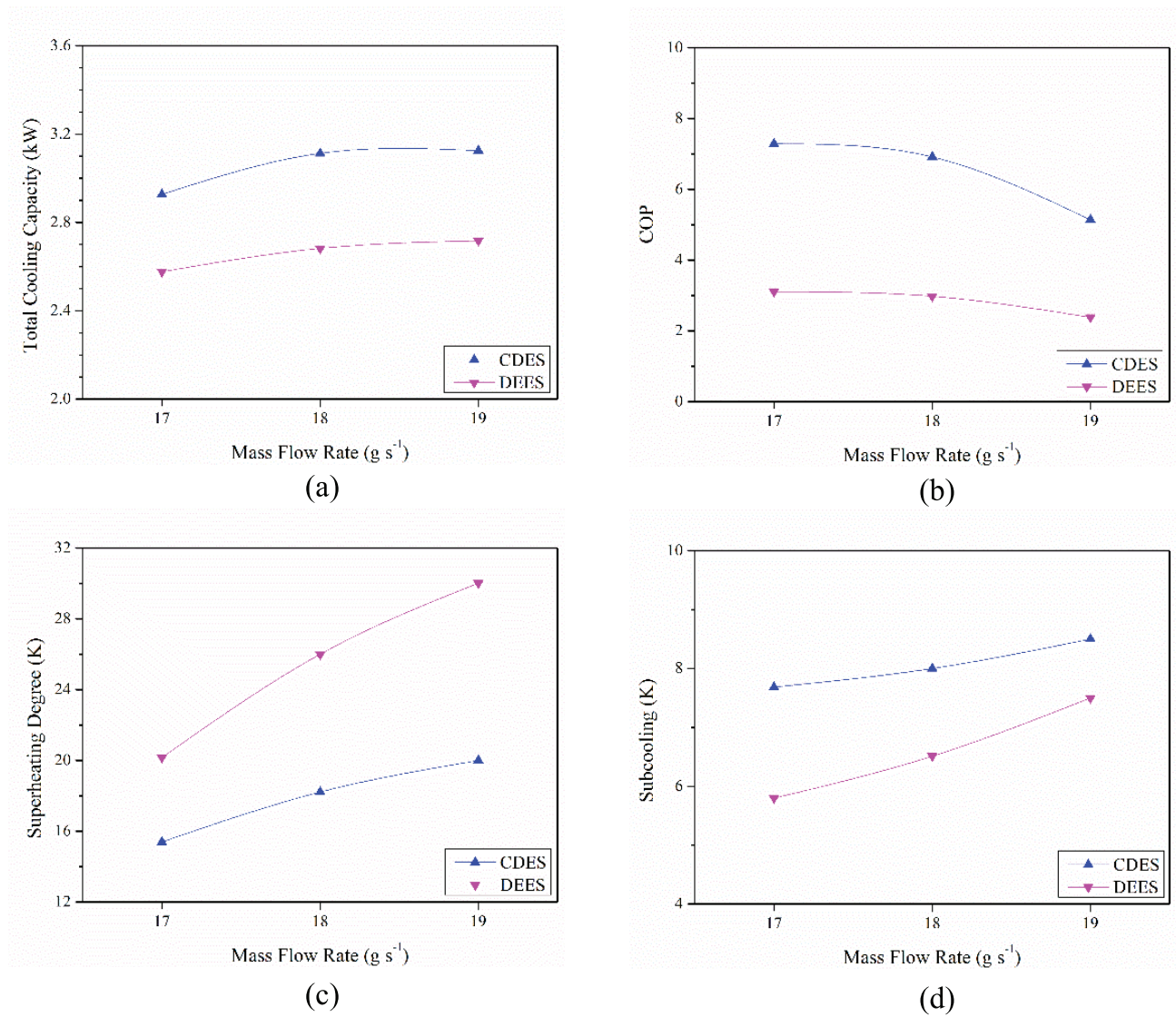


Figure 7. Changes in total cooling capacity (a) COP (b) superheating degree (c) and subcooling (d) as a function of mass flow rates.

The compressor inlet pressures increased in both configurations as the \dot{m}_r increased. For the same flow rate, the compressor inlet pressures measured in DEES were on average 10% lower than those of CDES (Figure 6a). Therefore, DEES operates at lower ct for the same flow rates. As depicted in Figure 3a, the use of an ejector results in an increase in the \dot{m}_r . When operating in CDES mode, the refrigerant needs to reach higher densities at the compressor inlet to achieve the same flow rates as those obtained in DEES mode. Therefore, in order to achieve the same flow rates, CDES mode requires higher compressor inlet pressures than DEES mode. The variation of the \dot{W}_{comp} for the two different configurations, depending on the \dot{m}_r , is shown in Figure 6b. \dot{W}_{comp} increased in both configurations with increasing \dot{m}_r .

The variation of the $\dot{Q}_{evap,total}$ of two different configurations depending on the \dot{m}_r is given in Figure 7a. In both configurations, the $\dot{Q}_{evap,total}$ increased with raising the flow rates. When operated at the same flow rate, the CDES mode achieved higher compressor inlet pressures and condenser temperatures compared to the DEES mode. Moreover, at higher condenser temperatures, the CDES mode provided a greater $\dot{Q}_{evap,total}$ than the DEES mode while maintaining the same flow rate. When the mass flow rate is 18 g/s, the $\dot{Q}_{evap,total}$ obtained in DEES mode is 2.6 kW, while it is 3.1 kW in the CDES mode. Similar results were observed for different COP values. It is detected that the COP values obtained from CDES for the same \dot{m}_r are higher than that of the DEES mode (Figure 7b). For the same flow rates, it was determined that the superheating degrees in DEES mode were higher than CDES (Figure 7c).

CONCLUSION

This study investigated the effect of the ejector on the performance parameters of an experimental refrigeration system, considering different configurations. The performance of the system was evaluated under various condensing temperatures and mass flow rates. Based on the results of the condenser temperature experiments, the DEES operating configuration exhibited the highest cooling capacity and COP values. The COP obtained from DEES was 15.9%, 6%, and 14.6% higher than the COP values obtained from the CDES, CVCR_A, and CVCR_B modes, respectively. The lowest cooling capacity and COP values were observed when the system was operated as CDES. At a condenser temperature of 33°C, the compressor power in the DEES mode was 22.7%, 5.4%, and 17.7% lower than the CVCR_A, CVCR_B, and CDES modes, respectively. At the same mass flow rate of 18 g/s, the compressor power required for DEES was 50% lower than that of CDES. Overall, the experimental parameters of the dual evaporator system operated with ejectors were found to be superior to the other configurations tested, and the ejector contributed positively to the system's performance. In future studies, the same

comparisons can be made using low GWP refrigerant alternatives instead of R134a.

NOMENCLATURE

h	Enthalpy, $kJ\ kg^{-1}$
i	Inlet
\dot{m}	Mass flow rate, $kg\ s^{-1}$
Q	Heat transfer, kW
Subscripts	
comp	Compressor
evap	Evaporator
r	Refrigerant

ACKNOWLEDGEMENTS

The authors are grateful to Yalova University (Project no: 2019-AP-0013 and 2021/YL/0020) for their supports.

AUTHORSHIP CONTRIBUTIONS

Authors equally contributed to this work.

DATA AVAILABILITY STATEMENT

The authors confirm that the data that supports the findings of this study are available within the article. Raw data that support the finding of this study are available from the corresponding author, upon reasonable request.

CONFLICT OF INTEREST

The author declared no potential conflicts of interest with respect to the research, authorship, and/or publication of this article.

ETHICS

There are no ethical issues with the publication of this manuscript.

REFERENCES

- [1] Dupont JL. The Role of Refrigeration in the Global Economy (2019), 38th Note on Refrigeration Technologies. Available at: <https://iifir.org/en/fridoc/the-role-of-refrigeration-in-the-global-economy-2019-142028>. Accessed February 21, 2024.
- [2] Bilir Sag N, Ersoy HK, Hepbasli A, Halkaci HS. Energetic and exergetic comparison of basic and ejector expander refrigeration systems operating under the same external conditions and cooling capacities. *Energy Convers Manag* 2015;90:184–194. [\[CrossRef\]](#)
- [3] Kutlu Ç, Ünal S, Erdinç MT. Thermodynamic analysis of Bi-evaporator ejector refrigeration cycle using R744 as natural refrigerant. *J Therm Eng* 2016;2:735–740. [\[CrossRef\]](#)

- [4] Caliskan O, Ersoy HK. Energy analysis and performance comparison of transcritical CO₂ supermarket refrigeration cycles. *J Supercrit Fluids* 2022;189:105698. [\[CrossRef\]](#)
- [5] Ünal Ş, Cihan E, Erdinç MT, Bilgili M. Influence of mixing section inlet and diffuser outlet velocities on the performance of ejector-expansion refrigeration system using zeotropic mixture. *Therm Sci Eng Prog* 2022;33. [\[CrossRef\]](#)
- [6] Zhang Z, Feng X, Tian D, Yang J, Chang L. Progress in ejector-expansion vapor compression refrigeration and heat pump systems. *Energy Convers Manag* 2020;207:112529. [\[CrossRef\]](#)
- [7] Tashtoush BM, Al-Nimr MA, Khasawneh MA. A comprehensive review of ejector design, performance, and applications. *Appl Energy* 2019;240:138–172. [\[CrossRef\]](#)
- [8] Lawrence N, Elbel S. Analytical and experimental investigation of two-phase ejector cycles using low-pressure refrigerants. *Int Refrig Air Cond Conf* 2012:1–11. [\[CrossRef\]](#)
- [9] Wang X, Yu J, Zhou M, Lv X. Comparative studies of ejector-expansion vapor compression refrigeration cycles for applications in domestic refrigerator-freezers. *Energy* 2014;70:635–642. [\[CrossRef\]](#)
- [10] Geng L, Liu H, Wei X, Hou Z, Wang Z. Energy and exergy analyses of a bi-evaporator compression/ejection refrigeration cycle. *Energy Convers Manag* 2016;130:71–80. [\[CrossRef\]](#)
- [11] Kim S, Jeon Y, Chung HJ, Kim Y. Performance optimization of an R410A air-conditioner with a dual evaporator ejector cycle based on cooling seasonal performance factor. *Appl Therm Eng* 2018;131:988–997. [\[CrossRef\]](#)
- [12] Gao Y, He G, Cai D, Fan M. Performance evaluation of a modified R290 dual-evaporator refrigeration cycle using two-phase ejector as expansion device. *Energy* 2020;212:118614. [\[CrossRef\]](#)
- [13] Liu J, Lu Y, Tian X, Niu J, Lin Z. Performance analysis of a dual temperature heat pump based on ejector-vapor compression cycle. *Energy Build* 2021;248:111194. [\[CrossRef\]](#)
- [14] Wang X, Yu J, Xing M. Performance analysis of a new ejector enhanced vapor injection heat pump cycle. *Energy Convers Manag* 2015;100:242–248. [\[CrossRef\]](#)
- [15] Wang M, Cheng Y, Yu J. Analysis of a dual-temperature air source heat pump cycle with an ejector. *Appl Therm Eng* 2021;193:116994. [\[CrossRef\]](#)
- [16] Chen J, Zhang G, Wang D. Experimental investigation on the dynamic characteristic of the direct expansion solar assisted ejector-compression heat pump cycle for water heater. *Appl Therm Eng* 2021;195:117255. [\[CrossRef\]](#)
- [17] Alkhulaifi YM, Qasem NAA, Zubair SM. Exergoeconomic assessment of the ejector-based battery thermal management system for electric and hybrid-electric vehicles. *Energy* 2022;245. [\[CrossRef\]](#)
- [18] İşkan Ü, Direk M. Experimental performance evaluation of the dual-evaporator ejector refrigeration system using environmentally friendly refrigerants of R1234ze(E), ND, R515a, R456a, and R516a as a replacement for R134a. *J Clean Prod* 2022;352. [\[CrossRef\]](#)
- [19] Ügüdü B. Experimental performance evaluation of the dual-evaporator ejector refrigeration system [Master's thesis]. Yalova: Yalova University; 2023 [Turkish].
- [20] Direk M, İşkan Ü, Tunçkal C, Mert MS, Yüksel F. An experimental investigation of ejector employed a dual-evaporator vapor compression refrigeration system under various entrainment ratios using R134a as the refrigerant. *Sustain Energy Technol Assess* 2022;52:102293. [\[CrossRef\]](#)